Dyna
ISSN: 0012-7353
dyna@unalmed.edu.co
Universidad Nacional de Colombia
Colombia

Graciano, Carlos; Martínez, Gabriela; Saavedra, Edwar
Effect of elastoplastic behavior on the impact response of expanded metal tubes
Dyna, vol. 83, núm. 198, septiembre, 2016, pp. 102-109
Universidad Nacional de Colombia
Medellín, Colombia

Available in: http://www.redalyc.org/articulo.oa?id=49647009012

How to cite
Complete issue
More information about this article
Journal's homepage in redalyc.org

Scientific Information System
Network of Scientific Journals from Latin America, the Caribbean, Spain and Portugal
Non-profit academic project, developed under the open access initiative

UNIVERSIDAD NACIONAL DE COLOMBIA
SEDE MEDELLÍN
FACULTAD DE MINAS

DYNA
http://dyna.medellin.unal.edu.co/

Effect of elastoplastic behavior on the impact response of expanded metal tubes

Carlos Graciano [a], Gabriela Martínez [b] & Edwar Saavedra [b]

[a] *Facultad de Minas, Universidad Nacional de Colombia, Medellín, Colombia, cagracianog@unal.edu.co*
[b] *Departamento de Mecánica, Universidad Simón Bolívar, Caracas, Venezuela, gabrielamb@usb.ve, saavedra.edwar@gmail.com*

Received: Abril 6th, 2015. Received in revised form: November 1rd, 2015. Accepted: March 25th, 2016.

Abstract
This paper presents a numerical study on the effect of the elastoplastic behavior of the material on the structural response of expanded metal tubes subjected to impact loads. The study is carried out using the finite element method, considering two material models. Firstly, a numerical model is built assuming a bilinear behavior with strain hardening. Secondly, a model is elaborated considering the speed of deformation using the correlation of Cowper-Symonds. These models are compared and validated with experimental results taken from the literature. Subsequently, a parametric study is conducted, varying the dimensions and orientation of the mesh as well as the impact speed. The results show that the response of expanded metal tubes is sensitive to changes in the orientation of the geometrical axes of the mesh. Increasing the dimensions of the strands increase the material available for plastic deformation, this, in turn, produces an increase in the energy absorbed per mass unit. In addition, the loading speed causes a delay in the response of the specimens.

Keywords: Expanded metal, Plasticity, Axial impact, Energy absorption, Dynamic response.

Efecto del comportamiento elastoplástico sobre la respuesta al impacto de tubos de metal expandido

Resumen
Este trabajo presenta un estudio numérico sobre el efecto del comportamiento elastoplastico del material sobre la respuesta estructural de tubos fabricados con mallas de metal expandido sometidos a cargas de impacto. El estudio se lleva a cabo utilizando el método del elemento finito, considerando dos modelos de material. En primer lugar, se elabora un modelo numérico asumiendo un comportamiento bilineal con endurecimiento por deformación. En segundo lugar, se emplea un modelo que considera la velocidad de deformación utilizando la correlación de Cowper-Symonds. Estos modelos son comparados y validados con resultados experimentales tomados de la literatura. Posteriormente, se lleva a cabo un estudio paramétrico variando las dimensiones y orientación de las mallas, y la velocidad de impacto. Los resultados muestran que la respuesta de los tubos de metal expandido es sensible a los cambios en la orientación de los ejes geométricos. Incrementando las dimensiones de las venas aumenta el material disponible para deformación plástica, lo cual a su vez produce un incremento en la energía absorbida por unidad de masa. Adicionalmente, la velocidad causa un retraso en la respuesta de los especímenes.

Palabras clave: Metal expandido, Plasticidad, Impacto axial, Absorción de energía, Respuesta dinámica.

1. Introduction

Many investigations have been conducted on devices designed to absorb energy during an impact scenario and therefore protect the structure in consideration [1]. An energy absorber is a system that converts, completely or partly, the kinetic energy into another form of energy, which can be either reversible or irreversible [2].

Since the second half of the twentieth century, there has been a remarkable growth in the number of vehicles on the roads. This has resulted in a large number of accidents and fatalities due to collisions and impacts that occur in various

How to cite: Graciano, C., Martínez G. & Saavedra E. Effect of elastoplastic behavior on the impact response of expanded metal tubes DYNA 83 (198) pp. 102-109, 2016.

© The author; licensee Universidad Nacional de Colombia.

ways. The need to improve the safety of vehicles and roads has led the scientific community to research and develop impact attenuation devices in order to absorb the kinetic energy of impacts and mitigate impacts on people and structures [3].

Significant state-of-the art reviews [2-4] in the field of crashworthiness have been conducted, summarizing over 40 years of research and developments of various types of collapsible structures that are designed to absorb kinetic energy during impact situations.

Nagel and Thambiratnam [1] used a finite element model to compare the response of conical and straight tubes subjected to impact loading tubes. They concluded that the lateral inertia of the tube affects the conical tubes less than the straight ones. Reid and Reddy [5] investigated the quasi-static and dynamic collapse of thin-walled tapered rectangular tubes. They developed analytical solutions of average for both collapse mode strengths. The dynamic solution took into account the effects of the strain-rate constitutive equation that was proposed by Cowper Symonds [6].

Wang and Lu [7] conducted experimental tests in which cylindrical tubes were impacted at speeds of about 300 m/s; their results showed a mushroom deformation mode. They mentioned that impacts at such high speeds are high complexity problems that can be analyzed only by numerical simulations and experimental tests.

Langseth et al. [8] performed finite element analyses on the collapse of square aluminum tubes. The numerical models were validated by comparing the results with experimental data from dynamic and quasi-static tests. It was concluded that, an increase in impact speed causes a significant increase in the breakdown strength. Hsu and Jones [9] performed quasi-static and dynamic tests on thin-walled tubes made with low carbon steel, stainless steel and aluminum alloys. The effects of strain-rate on material properties of the steel tubes were analyzed.

Rossi et al. [10] numerically analyzed the dynamic collapse of hexagonal extruded aluminum tubes with symmetric and asymmetric modes of collapse. They obtained good correlation with experimental results. Jones [11,12] classified the dynamic collapse of the tubes into two types: a) dynamic progressive buckling b) dynamic plastic buckling.

Recently, Graciano et al. [13-16] conducted a series of experimental and numerical investigations on the axial collapse of expanded metal tubes under quasi-static loading. It was found that expanded metal tubes under certain configurations may undergo a progressive and stable collapse and failure. Nouri et al. [17-18] performed a series of experimental and numerical studies on flattened expanded metal tubes that were subjected to impact.

In spite of the amount of research on the impact behavior of thin-walled structural member, expanded metal tubes under impact loading has received little attention. Hence, this research aims to investigate the effect of the elastoplastic behavior of the material on the impact response of expanded metal tubes. This investigation was carried out by means of nonlinear finite element analysis, and the numerical models are validated using results taken from the relevant literature. Thereafter, a parametric analysis is performed in order to investigate the influence of: a) two material models, a bilinear and strain-rate dependent model; b) the orientation of the expanded metal cells; and c) size of the cells on the impact response of the expanded metal tubes.

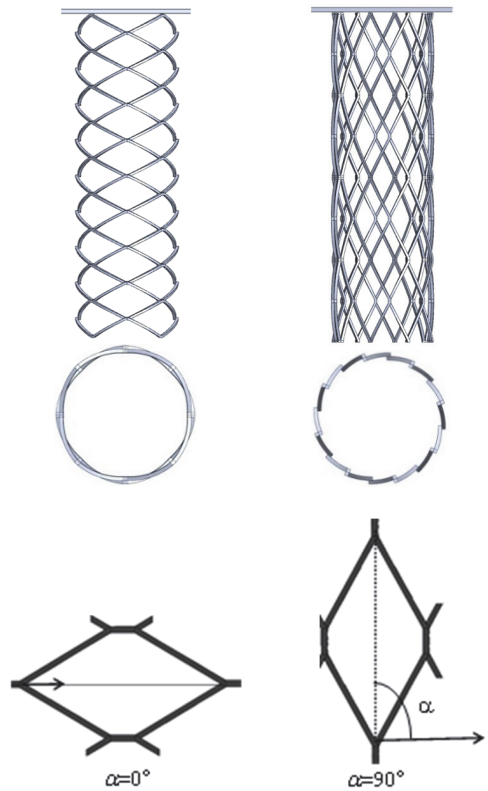

(a) (b)

Figure 1. Numerical models of expanded metal tubes.
Source: The authors.

2. Numerical model

2.1. Description

This section presents the development of a numerical model, using a finite element method for expanded metal tubes subjected to axial impact. The numerical analysis is conducted using the explicit analysis software ANSYS LS-DYNA [19]. The expanded metal cells in the tube were modeled with hexahedral high order SOLID 164 elements [19] that are suitable for large strain analyses. Two mesh orientations are considered in the analysis, one with α = 0° (Fig. 1a), and another with α = 90 ° (Fig. 1b).

Fig. 2 shows a schematic view of an EM cell; the pattern is characterized by a rhomb like shape. Table 1 presents the dimensions of the strands and cells used in the analysis. All tubes have an average length L= 400 mm, with a diameter ϕ = 120 mm. In general, the models were built depending on the cell orientation, for α = 0° the models have 4 cells in the circumferential direction and 9 cells in the longitudinal (Fig. 1a). For α=90° the models have 8 cells in the circumferential direction and 4 cells in the longitudinal (Fig. 1b).

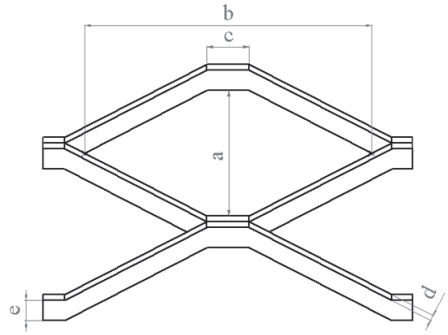

Figure 2. Nomeclature for EM cells.
Source: The authors.

Table 1.
Dimensions used in the parametric analysis.

Cell	*a* [mm]	*b* [mm]	*d* [mm]	*e* [mm]
H-24	44.70	90.00	1.90	2.80
H-26	44.20	89.60	3.00	3.20
H-27	36.80	81.60	6.00	6.00

Source: The authors.

The impact condition is generated using plates separated 1 mm from the upper end of the tube (Fig. 3a), which were modeled as a rigid body with a fixed mass *M*=20 kg. Initially, the rigid plate has an initial speed in the axial direction of the tube that causes axial impact. At the lower end the test specimen is clamped (Fig. 3b), *i.e.* it has all the degrees of freedom are fixed.

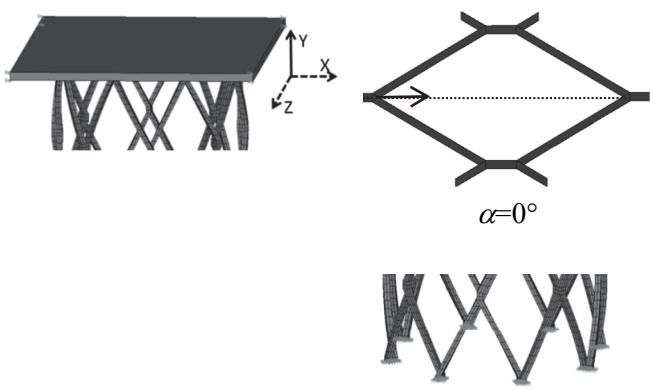

(a) Top end (b) Bottom end
Figure 3. Boundary conditions.
Source: The authors.

The material used was an ASTM A569 steel; however, two material models are used to investigate their effect on the elastoplastic response of the expanded metal tubes under impact:

Model 1: classical bilinear isotropic hardening model (strain-rate independent) that uses two slopes (elastic and plastic) to represent the stress–strain behavior of the material [20]. It has the following mechanical properties: Young's modulus E = 205 GPa; Poisson's ratio ν = 0.3; density ρ = 7835 kg/m^3; yield strength σ_y = 250 MPa; tangent modulus E_t = 660 MPa.

Table 2.
Material properties used for validation.

E [GPa]	ν	ρ [kg/m^3]	σ_y [MPa]	E_t [MPa]
207	0.3	7385	330	892

Source: Adapted from [1].

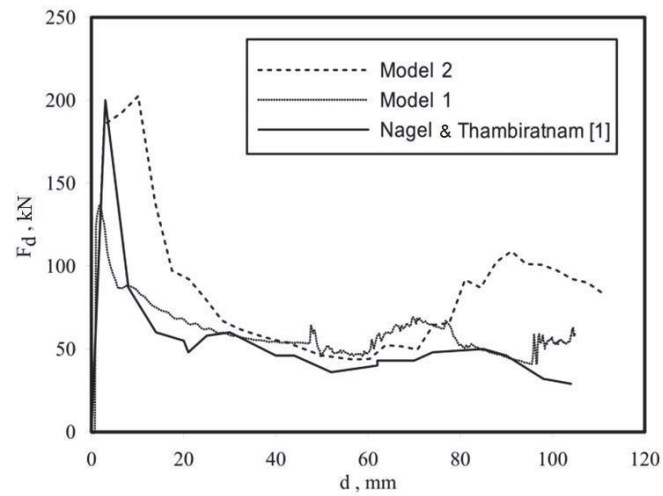

Figure 4. Load-displacement responses (Validation).
Source: The authors.

Model 2: considering dynamic effects, the dynamic yield strength needs to be calibrated depending on the deformation speed with Eq. (1). For carbon steels, the experimentally determined values [21] for the coefficients c and P are: c = 6844, and P = 3.91.

$$\sigma_{yd} = \sigma_y \left[1 + \left(\frac{\dot{\varepsilon}}{c} \right)^{1/P} \right] \quad (1)$$

2.2. Validation

The numerical procedure is validated by comparing the experimental and numerical results obtained by Nagel and Thambiratnam [1]. The geometry used was a rectangular solid tube with the following measurements: 48.31mm x 79.88mm, length L= 199mm and a thickness t= 1.5 mm. Table 2 shows the material properties employed. The tubes were subjected to an impact mass M= 90 kg, at a speed v= 15m/s. Due to symmetry in loading, geometry and boundary conditions, only one-fourth of the geometry was modeled.

Fig. 4 shows a comparison of the load–displacement responses obtained in [1] and those computed using the two material models depicted in the previous section, namely Model 1 and Model 2. It was observed that the best agreement with the experimental response from [1] was attained with Model 2. It is important to note that, in this case, Model 1 was unable to fully capture dynamic effects such as those presented in impact scenarios

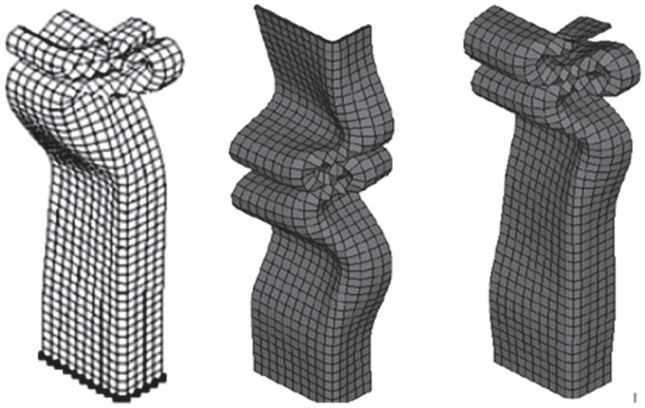

a) Taken from [1] b) Model 1 c) Model 2

Figure 5. Comparison of the deformed shapes for the straight tubes.
Source: The authors.

Comparing the peak loads for the three models, it seems that the best agreement is also achieved with Model 2. The peak load computed in [1] was P_{peak} = 200 kN; the corresponding for Model 1 is P_{peak} = 136.84 kN, for Model 2 it is P_{peak}= 202.46 kN. By using Model 1, the peak load is considerably underestimated.

Fig. 5 shows the deformed shapes obtained using the two material models. Once again, the results obtained with Model 2 (Fig. 5c) best agree with those attained in [1] (Fig. 5a). The deformation patterns appear rather close to the applied load. Additionally, for Model 1, a larger deformation occurs in the middle of the tube.

It is important to point out that the authors in [1] use a shell element formulation. The numerical model developed herein makes use of a solid element formulation. Recent studies have demonstrated an enhanced capability of the latter to represent impact effects in comparison to the former [22].

3. Parametric analysis

The numerical procedure was validated in the previous section with solid tubes [1]. A convergence analysis was conducted to calibrate the model for expanded metal tubes, hence a mesh with 8605 elements was chosen for the tubes with $\alpha = 0°$, and 7169 elements for $\alpha = 90°$ [21].

Next, a parametric study was conducted in order to investigate the influence of geometric variables on the impact response of expanded metal tubes:

(a) cell orientation (0 ° and 90 °);

(c) the loading speed (v =10, 15, 25, 35, 45, 50 m/s), and

(b) cell dimensions (see Table 1)

Load-displacement responses, deformed patterns at various displacement levels, and the energy absorption characteristics were the output parameters of the experimental investigation. To measure the energy absorption capacity, the following parameters were calculated: initial peak load (F_{peak}), mean load (F_m), absorbed energy (E_{200}), specific energy absorbed (E_e), and the structural efficiency (η).

The absorbed energy is primarily calculated by integrating the load-displacement curves, such as:

$$E_{200} = \int_0^{l_c} F dl \tag{2}$$

where F is the measured force and l_c is the crushing length. The mean force F_m based on the area under the curve over the crushing distance l_c is calculated by:

$$F_m = \frac{\int_0^{l_c} F dl}{l_c} \tag{3}$$

Afterward, the specific energy absorbed (E_e) was calculated by dividing the absorbed energy E_{200} by its weight W, according to:

$$E_e = \frac{E_{200}}{W} \tag{4}$$

Finally, the structural efficiency, defined as the ratio between the mean and the peak force is calculated by:

$$\eta = \frac{F_m}{F_{peak}} \tag{5}$$

All these parameters were calculated up to a crushing length l_c=200 mm.

3.1. Influence of the mesh orientation (α)

The load-displacement responses for the tubes with cells oriented at $\alpha = 0°$, and $\alpha = 90°$ are shown in Figs. 6a and 6b, respectively. In this analysis, a mesh type H-26 (Table 1) was used, the speed was v=15 m/s, and the mass was M= 20 kg.

From the load-displacement responses plotted in Fig. 6a, it can be observed that tubes with $\alpha = 0°$ exhibit a stable and controlled response, which is desirable for energy absorption purposes. In contrast, Fig. 6b shows rather instable behavior for tubes with $\alpha = 90°$. Regarding material behavior, Model 2 offers a greater resistance to the applied load than Material 1, and this effect is translated into a higher proportion of energy absorbed (see Table 3).

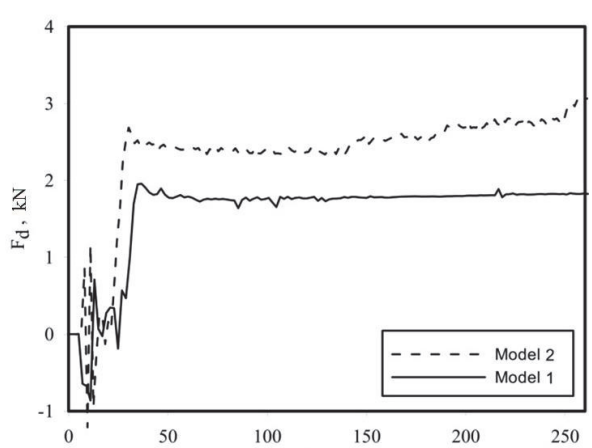

(a) $\alpha = 0°$

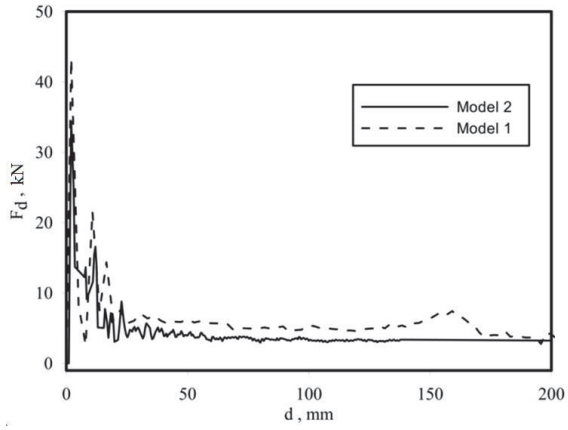

(b) $\alpha = 90°$

Figure 6. Load-displacement responses (mesh H-26 v=15 m/s).
Source: The authors.

Table 3.
Effect of the strand cross section.

	Model	F_{peak} [kN]	F_m [kN]	E_{200} [J]	η
0°	1	1.96	1.59	318.50	0.81
	2	2.69	2.29	458.21	0.85
90°	1	34.41	4.30	859.71	0.12
	2	43.29	5.98	1195.58	0.14

Source: The authors.

Table 3 summarizes the results for peak loads F_{peak}, mean loads F_m, energy absorbed E_{200}, and crush efficiency η for both the material models and the geometries analyzed herein. The tubes with $\alpha = 90°$ achieved a peak load up to 17 times greater than that for tubes with $\alpha = 0°$. At the same time, their mean load was just about 2.7 times higher than for $\alpha = 0°$. Nevertheless, the latter exhibits a better plastic performance and stability, which was shown in its crush efficiency that was close to 1. Moreover, the tubes with $\alpha = 90°$ absorb much more energy despite their instability: until almost 3 times more than the tubes with $\alpha = 0°$.

3.2. Influence of the loading speed

3.2.1. Tubes with $\alpha = 0°$

The impact speed varied from 10 m/s to 50 m/s. The nonlinear impact responses of the tubes with $\alpha = 0°$ for the two material models are plotted in Fig. 7. The mesh geometry corresponds to type H26, according to Table 1.

From the responses plotted in Fig. 7, it can be observed that an increase in impact speed leads to a decrease in the energy absorption capacity within the studied crushing length. This may be because during the process of cutting and stretching of the meshes, the loading direction is aligned with the corresponding direction of deformation, and, therefore, the cells collapsed more easily in this direction.

It is also observed that an increasing speed leads to a delay in the load-displacement responses, thus the amount of energy absorbed is reduced.

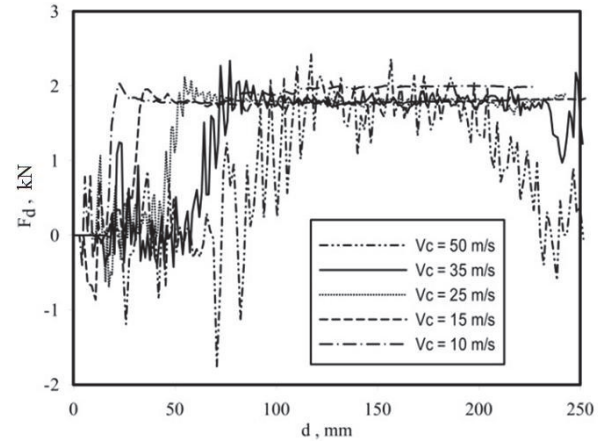

(a) α=0°/ Material Model 1

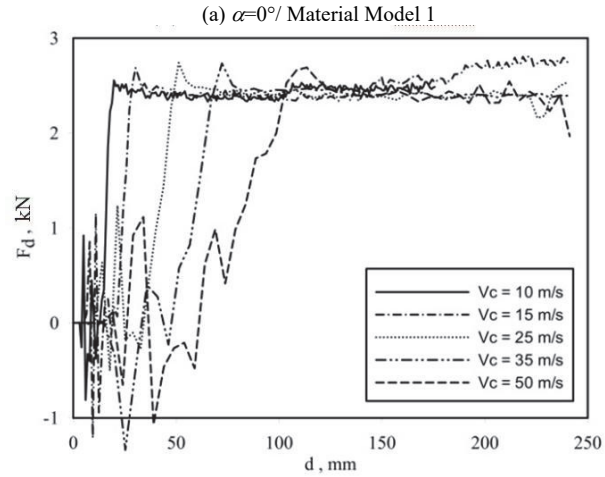

(b) α=0°/ Material Model 2

Figure 7. Effect of the loading speed α=0°.
Source: The authors.

As seen in Fig 8a, for speeds ranging from 10 m/s to 25 m/s, the cell collapses mainly in the middle part of the tube; this plastic behavior is more similar to the quasi-static case, as obtained in [13-16,22,23]. Furthermore, for higher speeds, from 35 m/s up to 50 m/s (Fig. 8b) the collapse propagates throughout the whole tube.

To summarize, the collapse modes of this configuration, within the investigated speed ranges, are dominated by local crushing of the cells.

3.2.1. Tubes with $\alpha = 90°$

The tubes' nonlinear impact responses, with α = 90° for the two material models, are plotted in Fig. 9. The mesh geometry corresponds to type H26 (Table 1). In this case, the strain-rate effects are also evidenced in the load-displacement responses, which are enhanced by the energy absorption characteristics that are observed after comparing the responses for Material 1 (Fig. 9a) and for Material 2 (Fig. 9b).

Furthermore, it can be observed that increasing speed produces an increase in the energy absorbed, in contrast to the previous case with α = 90°. This leads to the conclusion that the orientation of the cell produces different effects in the structural responses, with respect to changes in the loading speed.

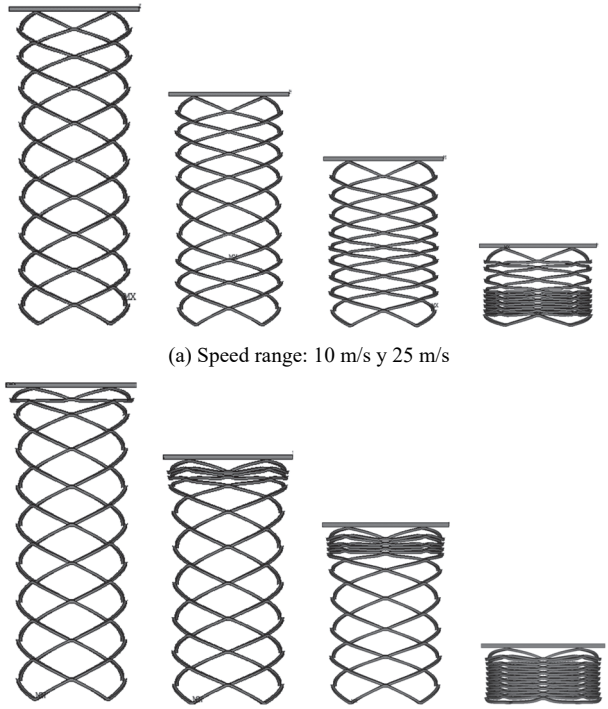

(a) Speed range: 10 m/s y 25 m/s

(b) Speed range: 35 m/s y 50 m/s

Figure 8. Progressive collapse for various speed ranges (α=0° - Model 2).
Source: The authors

Fig. 10a shows that at collapse, for speeds ranging from 10 m/s to 25 m/s, tubes with α =90° exhibit a widening in the middle, which originates from a buckling of the strands in the cells. This widening reaches its limit when the cells already involved are completely crushed, and results in the formation of a rigid circular ring near the middle section. Thereafter, the adjacent cells undergo progressive crushing. This ring reached a diameter of approximately two (02) times the initial tube diameter, as shown in Fig. 10a. Moreover, after the ring is shaped, the deformation of the specimen stops in the radial direction. It then begins to collapse axially through a combining crushing and buckling process of the cells, starting with those closest to the ring.

The deformation pattern changes for speeds ranging from 35 m/s up to 50 m/s (Fig. 10b). It can clearly be observed that, as the speed increases, the area of maximum deflection, due to local buckling, is the one closer to the impact zone. At low speeds, it approaches the area in the middle of the specimen (Fig. 10a). This seems reasonable, since in crash situations local deformation is first manifested in the impact zone: similar to the mushroom pattern observed for circular solid tubes in [7]. In the final crushing state, the load is transmitted throughout the whole structure.

3.3. Influence of the cell dimensions

In order to study the influence of the cell dimensions, three geometries are used in the analysis: namely H-24, H-26, and H-27A (Fig. 11). Both, the impact speed and mass remain constant: v=15 m/s, and *M*=20 kg. In this analysis, only material Model 2 is considered.

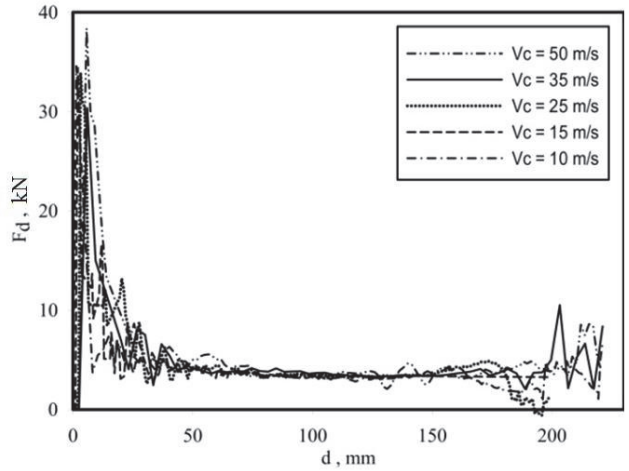

(a) 90°/ Material Model 1

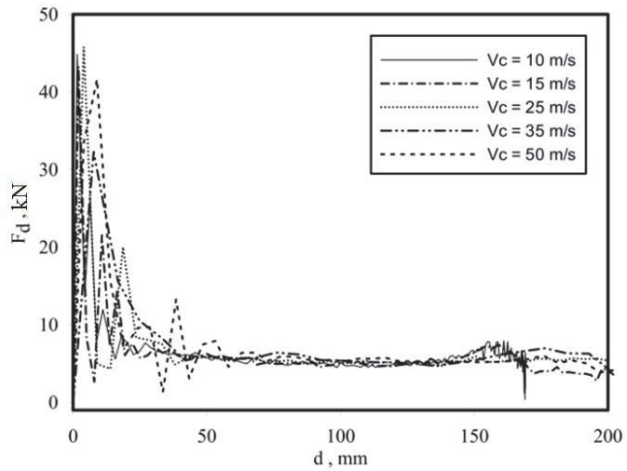

(b) 90°/ Material Model 2

Figure 9. Effect of the loading speed α=90°.
Source: The authors

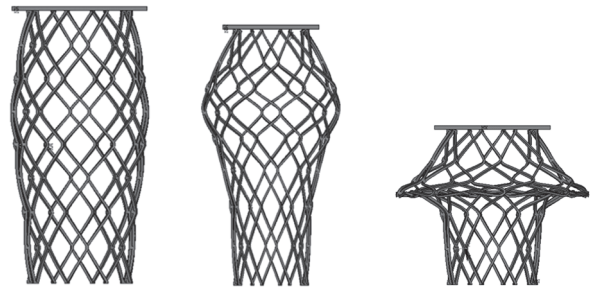

(a) Speed range: 10 m/s y 25 m/s

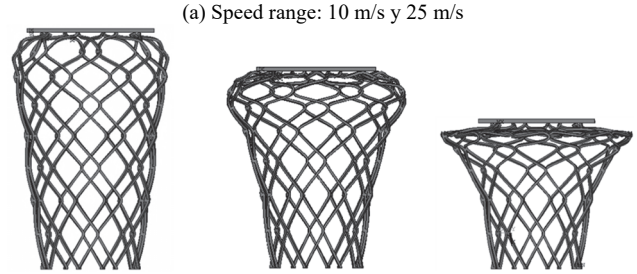

(b) Speed range: 35 m/s y 50 m/s

Figure 10. Progressive collapse for various speed ranges (α=90°-Model 2).
Source: The authors

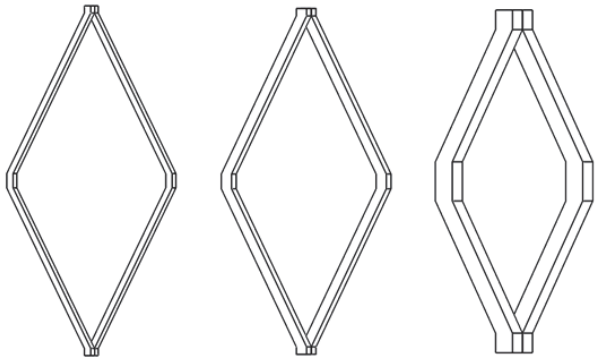

H-24 H-26 H-27A

Figure 11. Cell sizes used in the analysis.
Source: The authors

Table 4.
Effect of the strand cross section.

α	Model	W [kg]	F_p [kN]	F_m [kN]	E_{200} [J]	E_e [J/kg]
0°	H-24	0.294	1.8	1.22	244.48	831.56
	H-26	0.508	2.69	2.29	458.21	901.99
	H-27A	1.068	19.14	15.25	3050.13	2855.9
90°	H-24	0.261	20.73	2.81	562.79	2156.3
	H-26	0.451	43.29	5.98	1195.58	2650.9
	H-27A	0.949	145.29	35.86	7172.22	7557.7

Source: The authors

Increasing the dimensions of the cross-section of the strands increases their bending strength; it can be expected that the impact strength also increases. Moreover, Table 4 shows that this increase in strength is very sensitive to changes in dimensions, for instance, the cross section for mesh H-27A is 3.75 times larger than for mesh H-26, but the increase in the mean loads increases from 6.5 times for α = 90°, to 7 times for α =0°.

Consequently, the absorbed energy per the tubes' unit mass increases, which is highly convenient when designing compact, lightweight and economic energy absorbing systems that are of great the interests for the automotive industry (guardrails and crash attenuators). Table 4 shows these values and manifests the energy per unit mass (E_e) or specific energy.

4. Conclusions

This paper investigated the effect of the elastoplastic behavior of the material on the impact response of expanded metal tubes. Two material models, one bilinear with strain hardening and other depending on strain-rate were analyzed. We observed that the best results were achieved for the strain-rate dependent model (Model 2). Regarding the failure mechanism, we observed that at low-speed ranges impact scenarios the mechanism is similar to the one observed in quasi-static testing. Conversely however, for high-speed ranges the failure mechanism changes substantially; the failures occur rather close to the impact zone and then propagate to the bottom of the tubes. This conclusion is valid for the two cell orientations that were investigated in this paper. In addition, an increase in the cell cross section leads to a higher degree of the expanded metal tubes' energy absorption capacity.

References

[1] Nagel, G.M. and Thambiratnam, D.P., A numerical study on the impact response and energy absorption of tapered thin-walled tubes. International Journal of Mechanical Sciences, 46(2), pp. 201-216, 2004. DOI: 10.1016/j.ijmecsci.2004.03.006.

[2] Alghamdi, A.A.A., Collapsible impact energy absorbers: An overview, Thin-Walled Structures, 39(2), pp. 189-213, 2001. DOI: 10.1016/S0263-8231(00)00048-3.

[3] Olabi A.G., Morris, E. and Hashmi, M.S.J., Metallic tube type energy absorbers: A synopsis, Thin-Walled Structures, 45(7-8), pp. 706-726, 2007. DOI:10.1016/j.tws.2007.05.003.

[4] Qiu, X.M. and Yu, T.X., Some topics in recent advances and applications of structural impact dynamics. Applied Mechanic Review, 64(3), pp. 1-12, 2011. DOI: 10.1115/1.4005571.

[5] Reid, S.R. and Reddy, T.Y., Static and dynamic crushing of tapered tubes of rectangular cross-section, International Journal of Mechanical Sciences, 28(9), pp. 623-637, 1986. DOI: 10.1016/0020-7403(86)90077-9.

[6] Cowper, G.R. and Symonds, P.S. Strain-hardening and strain-rate effects in the impact loading of cantilever beams, Brown University Providence, R. I., nº TR-C11-28, 1957.

[7] Wang, B. and Lu, G., Mushrooming of circular tubes under dynamic axial loading, Thin-Walled Structures, 40(2), pp. 167-182, 2002. DOI: 10.1016/S0263-8231(01)00057-X.

[8] Langseth, M., Hopperstad, O. and Berstad, T., Crashworthiness of aluminium extrusions: Validation of numerical simulation, effect of mass ratio and impact velocity, International Journal of Impact Engineering, 22(9-10), pp. 829-854, 1999. DOI: 10.1016/S0734-743X(98)00070-0.

[9] Hsu, S. and Jones, N., Quasi-static and dynamic axial crushing of thin-walled circular stainless steel, mild steel and aluminum alloy tubes, International Journal of Crashworthiness, 9(2), pp. 195-217, 2004. DOI: 10.1533/ijcr.2004.0282

[10] Rossi, A., Fawaz, Z. and Behdinan, K,. Numerical simulation of the axial collapse of thin-walled polygonal section tubes, Thin-Walled Structures, 43(10), pp. 1646-1641, 2005. DOI: 10.1016/j.tws.2005.03.001

[11] Jones, N., Energy-absorbing effectiveness factor. International Journal of Impact Engineering, 37, pp. 754-65, 2010. DOI: 10.1016/j.ijimpeng.2009.01.008

[12] Jones, N., Structural Impact, New York: Cambridge University Press, 2011.

[13] Graciano, C., Martínez, G. and Smith, D., Experimental investigation on the axial collapse of expanded metal tubes, Thin-Walled Structures, 47, pp. 953-961, 2009. DOI: 10.1016/j.tws.2009.02.002

[14] Graciano, G., Martínez, G. and Gutiérrez, A., Failure mechanism of expanded metal tubes under axial crushing. Thin-Walled Structures, 51, pp. 20-24, 2012. DOI: 10.1016/j.tws.2011.11.001

[15] Martínez, G., Graciano, C. and Teixeira, P., Energy absorption of axially crushed expanded metal tubes. Thin-Walled Structures, 71, pp. 134-146, 2013. DOI: 10.1016/j.tws.2013.05.003

[16] Smith, D., Graciano, C. and Martínez, G., Quasi-static axial compression of concentric expanded metal tubes. Thin-Walled Structures, 84, pp. 170-176, 2014. DOI: 10.1016/j.tws.2014.06.012

[17] Nouri, M.D., Hatami, H. and Jahromi, A.G., Experimental and numerical investigation of expanded metal tube absorber under axial impact loading. Structural Engineering & Mechanics, 54(6), pp. 1245-1266, 2015. DOI: 10.12989/sem.2015.54.6.1245

[18] Hatami, H. and Nouri, M., Damghani. Experimental and numerical investigation of lattice-walled cylindrical shell under low axial impact velocities. Latin American Journal of Solids and Structures, 12(10), pp. 1950-1971, 2015. DOI: 10.1590/1679-78251919

[19] ANSYS LS-DYNA user's guide release 12.0 (2009).

[20] Sánchez, R., Determinación de las propiedades mecánicas de láminas de metal expandido. MSc. Tesis, Coordinación de Postgrado en Ingeniería Mecánica, Universidad Simón Bolívar, Caracas, Venezuela.

[En línea]. 2005. Disponible en: http://159.90.80.55/tesis/000129658.pdf
[21] Abramowics, W. and Jones, N., Dynamic progressive buckling of circular and square tubes. International Journal of Impact Engineering, 4(4), pp. 243-270. 1986. DOI: 10.1016/0734-743X(86)90017-5
[22] Kohar, C., Mohammadi, M., Raja, K. Mishra, R.K. and Inal, K., Effects of elastic-plastic behaviour on the axial crush response of square tubes. Thin-Walled Structures, 93, pp. 64-87. 2015. DOI: 10.1016/j.tws.2015.02.023 2015.
[23] Saavedra, E., Estudio numérico de estructuras fabricadas con mallas de metal expandido sometidas a cargas de impacto. Proyecto Final, Coordinación de Ingeniería Mecánica, Universidad Simón Bolívar, Caracas, Venezuela, [En línea]. 2011. Disponible en: http://159.90.80.55/tesis/000152468.pdf
[24] Smith, D., Estudio experimental de estructuras fabricadas con láminas de metal expandido sometidas a compresión axial. MSc. Tesis, Coordinación de Postgrado en Ingeniería Mecánica, Universidad Simón Bolívar, Caracas, Venezuela, [En línea]. 2008. Disponible en: http://159.90.80.55/tesis/000144470.pdf
[25] Gutiérrez, A., Análisis de los mecanismos de falla en estructuras de metal expandido sometidas a compresión. MSc. Tesis, Coordinación de Postgrado en Ingeniería Mecánica, Universidad Simón Bolívar, Caracas, Venezuela, 2010.

C. Graciano, received both his BSc. in 1992 and MSc. in 1995, in Mechanical Engineering from the Simon Bolivar University, Cafracas, Venezuela. He later moved to Sweden where he obtained a Licentiate of Engineering in 2001 and a PhD. in 2002, in Structural Engineering from Chalmers University of Technology and Luleå University of Technology, respectively. From 1997 to 2013, he served as assistant, associate and full professor in the Mechanical Engineering Department at the Simon Bolivar University, Caracas, Venezuela. Currently, he is an associate professor in the Civil Engineering Department at the Universidad Nacional de Colombia - Medellin campus. His research interests include: finite element modeling, structural stability, piping stress analysis and crashworthiness among others. ORCID: 0000-0003-0659-7963.

G. Martínez, received a BSc. in 1996 in Civil Engineering from the Universidad Francisco de Miranda in Coro, Venezuela, an MSc. in 2000 in Civil Engineering and a PhD. in 2005 in Mechanical Engineering from the Central University of Venezuela. She is currently a full professor in the Mechanical Engineering Department at the Simon Bolivar University, Caracas, Venezuela. Her research interests include: finite element modeling, biomechanics, structural stability and crashworthiness among others. ORCID: 0000-0003-0515-9400.

E. Saavedra, received a BSc. in 2011 in Mechanical Engineering from the Universidad Simon Bolivar, Caracas, Venezuela. He is currently a research assistant at the Universidad Simon Bolivar, in Caracas, Venezuela. His research interests include: finite element modeling, mechanical design, structural stability and crashworthiness among others.
ORCID: 0000-0002-1151-0677

UNIVERSIDAD NACIONAL DE COLOMBIA
SEDE MEDELLÍN
FACULTAD DE MINAS

Área Curricular de Ingeniería Mecánica

Oferta de Posgrados

Maestría en Ingeniería - Ingeniería Mecánica

Mayor información:

E-mail: acmecanica_med@unal.edu.co
Teléfono: (57-4) 4259262